THE ASTROPHYSICAL JOURNAL, 347:302–306, 1989 December 1

THE STRUCTURE OF THE INTERSTELLAR MEDIUM AT THE 25 AU SCALE

P. J. DIAMOND, W. M. GOSS, AND J. D. ROMNEY
National Radio Astronomy Observatory[1]
R. S. BOOTH
Onsala Space Observatory
AND
P. M. W. KALBERLA AND U. MEBOLD
Radioastronomsches Institut der Universität Bonn
Received 1989 April 14; accepted 1989 June 8

ABSTRACT

A three-station VLBI Galactic H I absorption experiment has been carried out with baselines up to 600 km. The large collecting area of the EVN (European VLBI Network) consisting of the Lovell Telescope, (Mark Ia) the 100 m telescope at Effelsberg and the Westerbork Synthesis Radio Telescope was necessary to achieve adequate sensitivity for these high angular resolution (0.″05) and high-velocity resolution (0.5 km s^{-1}) observations. The extragalactic sources 3C 138, 3C 147, and 3C 380 were observed. Changes in the local H I apparent absorption were observed in all three sources as a function of resolution. The changes are most striking in the direction of 3C 138. The implied linear diameters are in the range 25 AU with typical H I densities of 10^4–10^5 cm^{-3}.

Subject headings: interferometry — interstellar: matter — radio sources: 21 cm radiation

I. INTRODUCTION

Dieter, Welch, and Romney (1976) have observed the Galactic H I in the direction of 3C 147 ($l = 162°$, $b = 10°$) with a resolution of ~0.″1 using VLBI techniques. A single baseline between Hat Creek and Owens Valley was used in two observing sessions in 1973–1974 with a velocity resolution of 1 km^{-1}. Variations in the opacity of the zero velocity feature were observed as a function of interferometer hour angle. The observations implied that the H I opacity varies with a scale less than 0.″16. The authors state that an H I cloud of high density was observed "superposed on a slowly varying background." The cloud has a size less than 70 AU with an implied density of 10^5 cm^{-3} and a total H I mass of 3×10^{-7} $M_\odot$.

Subsequent observations by Dieter, Romney, and Backer (unpublished) used a three-station interferometer array to study the H I absorption in 3C 147 and five other sources. Although insufficiently sensitive to add new information, these measurements were consistent with the previously observed spatial gradient in H I opacity.

In 1981 August we observed galactic H I absorption in three extragalactic sources using the European VLBI Network. The purpose was to confirm the previous 3C 147 result and to extend the observations to two additional sources. The current results do confirm the Dieter *et al.* results and also show evidence for small scale structure in the H I interstellar medium in two additional directions.

II. OBSERVATIONS AND DATA REDUCTION

The observations were carried out in 1981 August using the three large radio telescopes of the EVN: the Jodrell Bank Lovell Telescope (Mark Ia-76 m), the Effelsberg 100 m telescope of the Max-Planck-Institut für Radioastronomie and the phased array of the Westerbork Synthesis Radio Telescope (WSRT) (equivalent to a 94 m antenna). The three baselines varied from 200 to 600 km in length.

We observed with the Mark II VLBI system, using a bandwidth of 250 kHz tuned to the frequency of H I adjusted for the LSR velocity of the absorbing clouds as determined from conventional interferometry. Some observations were performed with the receiver tuned 2 MHz away from the principal observing frequencies in order to calibrate the bandpass response function of the base band filters and the residual delay at each station. The data were correlated on the Mark II correlator of the Max-Planck-Institut für Radioastronomie in Bonn. We used the standard spectral line mode which produces a 196 channel cross-correlation function and two 96 channel autocorrelation functions for each baseline every second.

The first stage of the analysis was to average the cross-power data for 6 s and the autocorrelation data for one minute, principally to reduce the sheer bulk of the data. The data were then calibrated using the template spectrum method described by Diamond (1988); a high-quality total power spectrum (a template spectrum) was generated by averaging and Fourier transforming the autocorrelation functions from the Effelsberg dish. The spectra were then corrected for the effects of the bandpass filters using total power spectra of the continuum sources taken at a slightly different frequency. The bandpass-corrected power spectra from the other antennas were then fitted to the template spectrum using a least-squares algorithm. The fit generated so-called "quality factors" which are proportional to the relative areas, efficiencies and system temperature of the antennas. These relative calibration factors were then multiplied by the measured system temperature and gain of the Effelsberg antenna in order to produce the final calibration factors.

The cross-power data were then corrected for the effects of

[1] Associated Universities, Inc. operates the National Radio Astronomy Observatory under National Science Foundation Cooperative Agreement No. AST-8814515.

TABLE 1

SOURCES OBSERVED VLBI GALACTIC H I ABSORPTION

Name	Galactic Coordinates (l° b°)	Flux Density (Jy)	Observing Time (hr)	VLBI Size	Visibility (Short)	Visibility (Long)	References
3C 138.....	187.5, −11.3	9	2	0.″45	0.3–0.4	0.03–0.1	1
3C 147.....	161.7, 10.3	22	5	0.25	0.2–0.4	~0.07	2, 3
3C 380.....	77.2, 23.5	14	11	0.025	0.3–0.35	0.05–0.1	4

REFERENCES.—(1) Geldzahler *et al.* 1984. (2) Simon *et al.* 1983. (3) Readhead and Wilkinson 1980. Also extended structure of ~0.″6 (Wilkinson *et al.* 1984*a*). (4) Pearson and Readhead 1981. Also extended structure 3″–6″ (Wilkinson *et al.* 1984*b*).

the bandpass filters and multiplied by the calibration factors to produce calibrated cross-power spectra. These spectra were then read into AIPS (Astronomical Image Processing System of NRAO) for further calibration and analysis.

The final stage of the calibration was to determine the station based residual delays and fringe rates. We used the data at the offset frequency to determine the residual delay of each station. The data were corrected for the phase slopes across the band induced by the residual delays. In addition residual fringes-rates were determined from the data at the frequency of the absorption line. The data then were corrected for the effects of the residual fringes rates and a calibrated data set was produced. The coherence time was ~5 minutes and the theoretical rms noise was 0.02–0.04 Jy in 1 hr; however, the accuracy is limited by the bandpass calibration at the 2%–3% level.

The parameters of the three sources are summarized in Table 1. The continuum sizes and references to the continuum structures are listed. Typical continuum visibilities on the WSRT–Effelsberg baseline are listed (short) as well as values on one of the two long baselines to Jodrell Bank (Jodrell Bank to Effelsberg). Attempts were made to image the H I absorption relative to the background brightness distribution, using existing VLBI images of these well known sources at nearby frequencies to model the continuum emission. However, due to the limited observing times and UV coverage this imaging was not possible. The data analysis was based on visibility plots (amplitude vs. baseline length) and average spectra obtained with different baseline lengths. Since no images of the H I opacity are possible the conclusions are only semiquantitative. Future observations will ensure that the UV coverage is sufficient to image the H I absorption distributions.

III. RESULTS

a) 3C 147

The observational results are summarized in Figures 1–4. In Figure 1 (*box, top right*) the average spectra of 3C 147 (amplitude scalar averaged) for the entire observation are shown for two of the three baselines. The Effelsberg–WSRT spectrum with an average projected baseline of 200 km agrees with the single dish and short baseline interferometer spectra previously obtained (e.g., Mebold *et al.* 1981). At this resolution (fringe spacing 0.″2), the source of total size 0.″25 is

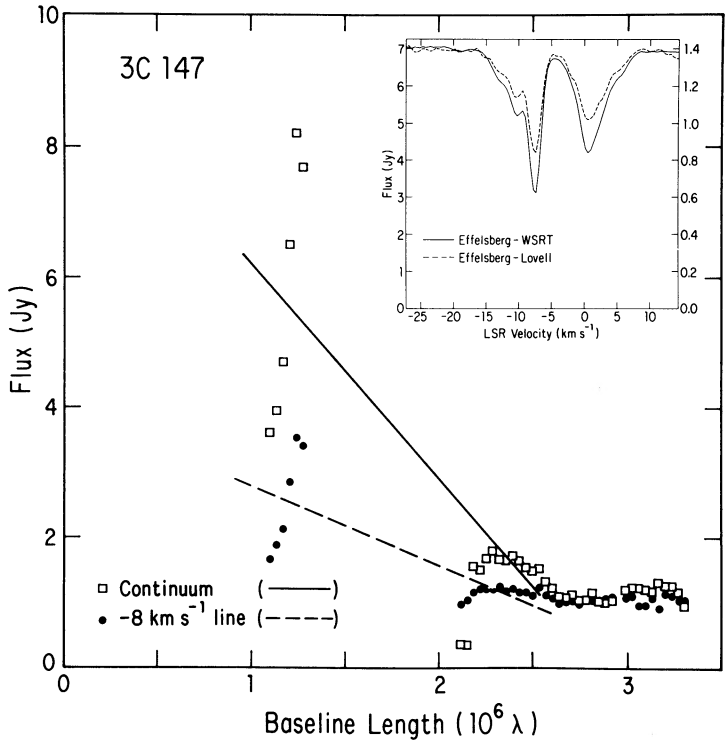

FIG. 1.—The visibility plot of the continuum (*open squares*) and absorption feature at −8 km s^{-1} (*filled circles*) for 3C 147. The solid and dashed lines indicate the respective average slopes. The box shows the scalar averaged cross-power spectra of 3C 147. The solid line is the spectrum measured on the Effelsberg–WSRT baseline; the flux density scale on the left is appropriate for this baseline. The dashed line is the spectrum measured on the Effeleberg–Jodrell Bank (Lovell) baseline; the flux density scale is given on the right. The spectra have been Hanning smoothed to a velocity resolution of 0.87 km s^{-1}. Velocity is with respect to lsr.

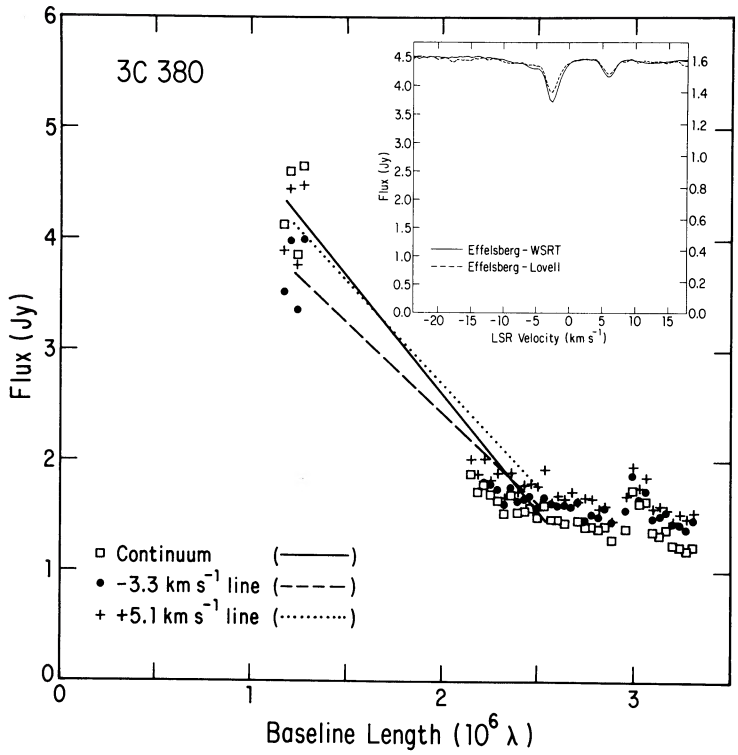

FIG. 2.—The visibility plot of the continuum (*open squares*), the absorption feature at −3.3 km s^{-1} (*filled circles*) and the absorption feature at 5.1 km s^{-1} (*plus signs*) for 3C 380. The solid line indicates the slope of the visibility for the continuum, the dashed line indicates the slope for the −3.3 km s^{-1} feature and the dotted line for the 5.1 km s^{-1} feature. The box shows the scalar-averaged cross-power spectra of 3C 380. The solid line is the spectrum measured on the Effelsberg–WSRT baseline; the flux density scale on the left is appropriate for this baseline. The dashed line is the spectrum measured on the Effelsberg–Jodrell Bank (Lovell) baseline; the flux density scale is given on the right. The spectra have been Hanning smoothed to a velocity resolution of 0.87 km s^{-1}.

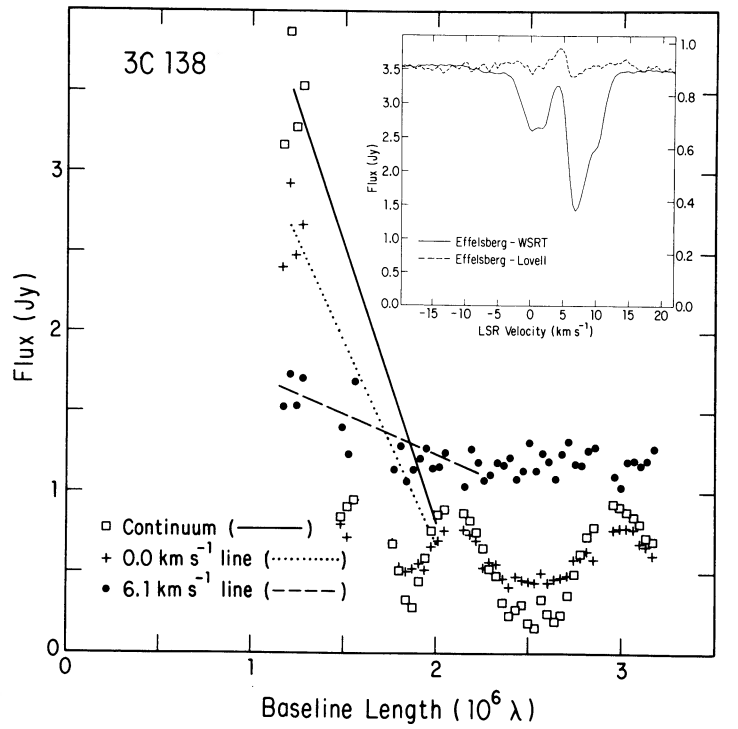

FIG. 3.—The visibility plots of the continuum (*open squares*), the shallow absorption feature at 0.0 km s^{-1} (*plus signs*) and the deep absorption feature at 6.1 km s^{-1} (*filled circles*). The solid line indicates the slope of the visibility for the continuum, the dotted line for the 0.0 km s^{-1} and the dashed line for the 6.1 km s^{-1} feature. The box shows the scalar averaged cross-power spectra of 3C 138 (averaged over the whole observing session). The solid line is the spectrum measured on the Effelsberg–WSRT baseline: the flux density scale on the left is appropriate for this baseline. The dashed line is the spectrum on the Effelsberg-Jodrell Bank (Lovell) baseline; the flux density scale is given on the right. The spectra have been Hanning smoothed to a velocity resolution of 0.87 km s^{-1}.

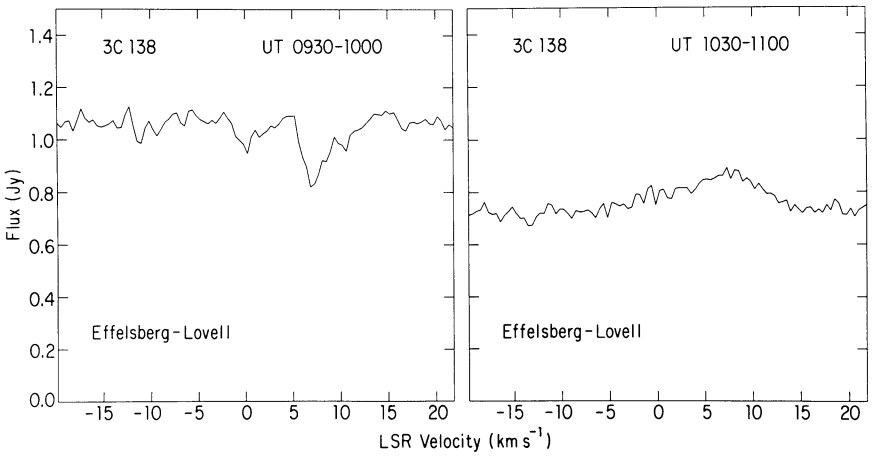

FIG. 4.—Scalar averaged cross-power spectra of 3C 138 on the Effeleberg–Jodrell Bank (Lovell) baseline. (*a*) The spectrum averaged over the period 0930–1000 UT, (*b*) The spectrum 1 hr later averaged over the period 1030–1100.

somewhat resolved and the visibility is in the range 0.3–0.4 (Table 1). The two longer baselines to Jodrell Bank are similar in length and the two averaged spectra agree to within the noise. The average Effelsberg to Jodrell spectrum is also shown as a dashed line in Figure 1. The shape of the spectra is similar but the line depth (as measured downward from the continuum level) to continuum ratios of the absorption lines on the longer baselines are smaller i.e., the H I absorption lines appear to be weaker on the long baselines as compared to the shorter 200 km baselines. As Radhakrishnan *et al.* (1972) have shown, the apparent weakening of the line depth with respect to the continuum is due to a nonuniform coverage of the continuum source by the intervening absorbing gas. The observed flux density in the line with respect to the continuum is higher, since the absorbed source is smaller in the presence of high optical depth clumps which cover the source in a nonuniform manner.

The 3C 147 visibility plots for the continuum and for the deepest H I line at -8 km s^{-1} are also shown in Figure 1. The different slopes of the visibilities in the line and continuum are obvious. The slopes are, of course, related to the effective angular size; the line source is smaller than the continuum in agreement with the spectra of 3C 147. Again it is apparent that the source is not covered in a uniform fashion by the intervening H I. The line at 0 km s^{-1} shows a similar behavior.

b) 3C 380

In Figure 2 similar spectra and visibility plots for 3C 380 are shown. As is the case for 3C 147, the Effelsberg–WSRT spectrum is identical to the short baseline spectrum published by Mebold *et al.* (1981) while the spectra on the two Jodrell Bank baselines show an apparent weaker line at $v = -3.3$ km s^{-1}. The line at 5.1 km s^{-1} is identical in the spectra on all three baselines, implying that at this velocity the coverage of the source is uniform for this range of angular scales. In Figure 2 the visibility plots for the continuum and deep line (-3.3 km s^{-1}) are also displayed, again showing the difference in angular sizes for the line and continuum. As is the case for 3C 147 the effective size of the source at the line velocity is smaller than the continuum. Also shown in Figure 2 is the visibility plot for the weaker line at 5.1 km s^{-1}; as can be seen its slope is similar to the continuum, consistent with the result provided by the spectra.

c) 3C 138

The results for 3C 138 are much more complex and will require additional observations to unravel the details of the H I opacity distribution. In Figure 3 the visibility plots and the spectrum for the WSRT–Effelsberg baseline are shown. Based on this spectrum, the line is considerably weaker on the 200 km baseline as compared to single dish or interferometer spectra with baselines of hundred of meters (Mebold *et al.* 1981). As an example, the apparent opacity for the 6.1 km s^{-1} line is 0.78 in the spectrum shown in Figure 3 as compared to 0.96 observed by Mebold *et al.* The VLBI structure is much larger than the other two sources ($\sim$0.″6; Geldzahler *et al.* 1984) and the typical visibility on the 200 km baseline is only 0.3.

On the longer baselines involving Jodrell Bank, the typical visibility is only 0.06. The H I spectra on the long baselines do not resemble the 200 km baseline spectrum shown in Figure 3. The spectra change rapidly as a function of projected baseline. Two sample spectra are shown in Figure 4 [obtained on the Effelsberg–Jodrell Bank (Lovell baseline)]. Figure 4*a* shows a weak "absorption" line while in Figure 4*b* (obtained $\sim$1 hr later) the line is apparently in emission. This effect has been observed earlier in galactic H I absorption at much lower angular resolutions. As an example Radhakrishnan *et al.* (1972) have observed Orion A (angular size $\sim$5′) with an interferometer spacing of 210 m and found that the line visibility is 4 times that of the continuum at a velocity of -2 km s^{-1}. If the source is heavily resolved by the interferometer and the opacities are large, the effective "absorbed source" will have a higher flux density than the "unabsorbed source" or continuum.

In summary, the VLBI H I observations with a 600 km baseline of 3C 147 and 3C 380 show that the two major low-velocity lines in 3C 147 and the strongest line in 3C 380 appear to be essentially scaled down versions of the 200 km observations. It is, indeed, puzzling that the shape of the H I lines have not changed as a function of resolution. This effect may be due to the fact that the small-scale structure is not heavily resolved.

For the source that is heavily resolved on the long baseline, 3C 138, the charges in the spectra at the 600 km baselines are dramatic. These data do not resemble the 200 km baseline or single dish data. At some hour angles, the source is covered in such a nonuniform manner that the line flux densities are larger than the continuum.

IV. DISCUSSION

In three directions the local galactic H I with a distance of less than $\sim$500 pc (based on a galactic latitude 10°–24° and an assumed height of the hydrogen layer above the plane of 100 pc) shows structure with angular sizes less than $\sim$0.″1. The

angular sizes implied by the visibility data for the three sources are $\sim 0''.05$. The typical linear dimensions for an object with such an angular size at 500 pc is 25 AU. The typical column density is 4×10^{19} cm^{-2} (based on an assumed spin temperature of 50 K) and the resultant densities are in the range $(5\text{–}10) \times 10^4$ cm^{-3}. These parameters are similar to those suggested by Dieter *et al.* (1976).

Based on this sample of three directions, it could be that such small condensations are a general property of the local interstellar medium. As Dieter *et al.* (1976) have stressed, these clouds are smaller by several orders of magnitude than previously observed H I clouds (e.g., Kalberla, Schwarz, and Goss 1985; Crovisier, Dickey, and Kazès 1985; Greisen and Liszt, 1986). The H I densities approach those observed in dense molecular clouds. Presumably the H I in these small condensations does not form H_2 with column densities of $\sim 10^{19}$–10^{20} cm^{-2} due to the lack of protection against the interstellar UV (Federman, Glassgold, and Kwan 1979; van Dishoeck and Black 1988). Further progress on the nature of these dense H I clouds awaits the direct imaging of the opacity distributions. A major question is the filling factor of these objects in the neutral interstellar medium.

An additional complication raised by these observations is that the pressure in the gas is 10^2–10^4 times greater than that of the average interstellar medium, implying that the compact structures observed are unstable and would tend to dissipate on time scales of ~ 100 yr. The small number statistics tend to argue against this short lifetime, in which case some confining or rapid regeneration mechanism is needed, It is unlikely that each compact object is bound to a star, since in the directions observed the number of compact absorbing objects must be less than $\sim 10^5$ pc^{-3}, i.e., $\sim 10^5$ times more common than the average stellar density. The energy required to maintain a constant number of clouds is $\sim 10^{42}$ ergs s^{-1}. This energy is equivalent to one supernova per 30 yr, and it seems unlikely that such an energy source lies in each of the directions observed. If a magnetic field were causing the confinement it would require a strength of ~ 200 μG, a value more than 20 times the field strengths so far observed in the average interstellar medium. However this field is similar to the 200 μG field observed in the bipolar molecular outflow region S106 (Kazès *et al.* 1988; R. Loushin, private communication).

There is the possibility that the current H I results are related to the extreme scattering events observed by Fiedler *et al.* (1987) or the rapid changes in the intensity of two compact extragalactic sources with time scales of hours (Quirrenbach *et al.* 1989). Fielder *et al.* suggest that the events were caused by compact (< 7 AU) objects within 1.3 kpc of the Sun moving at a transverse velocity of less than 200 km s^{-1} and that a given source is occulted $\sim 7 \times 10^{-3}$ of the time. These estimates do not appear to fit the H I data; however, further observations are required to examine this possibility.

An important question is the relationship of the small-scale H I structure as observed by VLBI techniques and the absorption observed against pulsars. Pulsars have angular sizes at 21 cm of 10^{-5}–10^{-4} arc seconds (due to scattering in the interstellar medium) and are thus much smaller than the compact extragalactic sources investigated here. Dickey *et al.* (1981) have demonstrated that the statistics of the H I opacity distributions are the same for pulsars as for extragalactic sources. Thus the covering factor of any set of optically thick concentrations must be of order unity, i.e., the interstellar medium does not consist of optically thick concentrations that cover only a small portion of the solid angle of the sources with an optically thin medium in between (Dickey *et al.* 1981). The current results indicate that there may be a continuous range of optically thick cloudlets with characteristic sizes of tens of AU.

We would like to thank R. T. Schilizzi for his assistance in organizing these observations. Nan Dieter provided enthusiastic encouragement in 1987–1989, and we thank her. We would also like to express our appreciation to Peter Wilkinson, Carla Fanti, and Richard Simon for providing us with continuum VLBI data, and to Joel Bregman, Don Backer, and John Dickey for interesting discussions. We thank the MPI correlator staff for assistance. The Westerbork Synthesis Radio Telescope is operated by the Netherlands Foundation for Research in Astronomy which is financially supported by the Netherlands Organization for Scientific Research (NWO).

REFERENCES

Crovisier, J., Dickey, J. M., and Kazès, I. 1985, *Astr. Ap.*, **146**, 223.
Diamond, P. J. 1988, in *Synthesis Imaging in Radio Astronomy*, ed. R. A. Perley, F. R. Schwab, and A. H. Bridle (San Francisco: Astronomical Society of the Pacific), p. 379.
Dickey, J. M., Weisberg, J. M., Rankin, J. M., and Boriakoff, 1981, *Astr. Ap.*, **101**, 332.
Dieter, N. H., Welch, W. J., and Romney, J. D. 1976, *Ap. J. (Letters)*, **206**, L113.
Federman, S. R., Glassgold, A. E., and Kwan, J. 1979, *Ap. J.*, **227**, 466.
Fielder, R. L., Dennison, B., Johnston, K. J., and Hewish, A. 1987, *Nature*, **326**, 675.
Geldzahler, B. J., Fanti, C., Fanti, R., Schilizzi, R. T., Weiler, K. W., and Shaffer, D. B. 1984, *Astr. Ap.*, **131**, 232.
Greisen, E. W., and Liszt, H. S. 1986, *Ap. J.*, **303**, 702.
Kalberla, P. M. W., Schwarz, U. J., and Goss, W. M. 1985, *Astr. Ap.*, **144**, 27.
Kazès, I., Troland, T. H., Crutcher, R. M., and Heiles, C. 1988, *Ap. J.*, **335**, 263.
Mebold, U., Winnberg, A., Kalberla, P. M. W., and Goss, W. M. 1981, *Astr. Ap. Suppl.*, **46**, 389.
Pearson, T. J., and Readhead, A. C. S. 1981, *Ap. J.*, **248**, 61.
Quirrenbach, A., Witzel, A., Krichbaum, T., Hummel, C. A., Alberdi, A., and Schalinski, C. 1989, *Nature*, **337**, 442.
Radhakrishnan, V., Brooks, J. W., Goss, W. M., Murray, J. D., and Schwarz, U. J. 1972, *Ap. J. Suppl.*, **24**, 1.
Readhead, A. C. S., and Wilkinson, P. N. 1980, *Ap. J.*, **235**, 11.
Simon, R. S., Readhead, A. C. S., Moffet, A. T., Wilkinson, P. N., Allen, B., and Burke, B. F. 1983, *Nature*, **302**, 487.
van Dishoeck, E. F., and Black, J. H. 1988, *Ap. J.*, **334**, 771.
Wilkinson, P. N., Spencer, R. E., Readhead, A. C. S., Pearson, T. J., and Simon, R. S. 1984*a*, in *VLBI and Compact Radio Sources* ed. R. Fanti, K. I. Kellermann, and G. Setti (Dordrecht: Reidel), p. 25.
Wilkinson, P. N., Booth, R. S., Cornwell, T. J., and Clark, R. 1984*b*, *Nature*, **308**, 619.

R. S. BOOTH: Onsala Space Observatory, S-430 34 Onsala, Sweden

P. J. DIAMOND and J. D. ROMNEY: National Radio Astronomy Observatory, Edgemont Road, Charlottesville, VA 22903

W. M. GOSS: National Radio Astronomy Observatory, P.O. Box 0, Socorro, NM 87801

P. M. W. KALBERLA: Radioastronomisches Institut der Universität Bonn, Auf dem Hügel 71, D-5300 Bonn 1, Federal Republic of Germany